ILASS 2008
Sep. 8-10, 2008, Como Lake, Italy

Paper ID ILASS08-7-8

EXPERIMENTAL ANALYSIS OF GLOBAL RAINBOW REFRACTOMETRY RESPONSE TO NON SPHERICAL DROPLETS: COMPLEMENTARITIES OF THREE OPTICAL TECHNIQUES

S. Saengkaew, G. Godard, J.B. Blaisot and G. Gréhan

LESP, UMR 6614/CORIA,
CNRS/INSA et Université de Rouen,
Avenue de L'université, BP 08
76 800 Saint Etienne du Rouvray, France

ABSTRACT

Sprays characterization asks to measure a large number of parameters as: particle size distribution, particle velocity, particle concentration, particle shape, particle temperature, particle composition, etc. For each of these parameters specific measurement strategies and associated devices have been developed along the years. Each of these techniques possesses its own advantages and limitations. Global Rainbow technique (GRT) is a promising technique used to measure the temperature of liquid droplet with few degrees of accuracy. Moreover, simultaneously to the temperature, this technique can also provide an estimation of the droplet size distribution. This paper is devoted to the comparison of the size distribution extracted from signals recorded by three different optical techniques (Shadow imaging, PDA and Global rainbow) from lines of droplet with a different level of non sphericity.

INTRODUCTION

The combustion of liquid necessitates their atomization as a spray of small droplets which evaporates. Schematically, for multicomponent droplets, this phenomenon is connected to the heat up of the droplets to the boiling point of the lighter product, the clearing of the lighter product, and the heat up to the boiling point of the next lighter product and so on.

Such a process can be modelized by several models and codes. Nevertheless, such codes depend a lot on physical parameters describing the product (which are not always very well known or can correspond to hundred of elementary components as for kerosene or bio diesel).

The measurement of the aerothermal properties of droplets in spray is a central problem for simple evaporation or combustion, with application to the design of modern combustion chambers of turbojet, automotive engines and rocket engines.

Several teams try to release this challenge by using different techniques as MDR [1], LIF [2], IR [3], spontaneous Raman scattering [4] or rainbow refractometry [5]. For all these techniques, to transform the recorded signal to temperature or evaporation rate, assumptions on the geometry of the droplets will be introduced as particle shape, gradient of temperature, gradient of composition, etc. Nevertheless, for physical and practical reasons, the particles are nearly all the time assumed to be perfectly spherical. According to the technique used, deviation from this reference shape can introduce large errors in the measurement.

For a perfectly spherical droplet, in the framework of geometrical optics, the angular location of the main rainbow is a monotonic function of its refractive index. As the refractive index is a function of the product temperature and composition, the measurement of the absolute angular location of the mean rainbow can be a measure of the droplet temperature or composition. This is the basic principle of rainbow refractometry.

However, real implementation of rainbow refractometry must take account of:

1. **The finite size of the droplet** which is at the origin of interference between once internally reflected rays. This is classically described by the Airy's theory.
2. **The interference of different kind of interactions** between the light and the droplet at the origin of high frequency components called ripple. The ripple is mainly due to the externally reflected light but other interactions can be significant.
3. **Possible of temperature or composition gradients inside the droplets** which induce a modification of the relationship between rainbow angular location and refractive index value.
4. **A shape different from the perfect sphere** which can induce a modification of the relationship between rainbow angular location and refractive index value.

When applied to an individual droplet, the rainbow location is very sensitive to any tiny departure from the perfectly spherical shape [6]. Then van Beeck et al [7] introduce the global rainbow refractometry where the synthetic rainbow created by the summation of a large number of individual rainbows is recorded. The global rainbow pattern is claimed to be insensitive to the non spherical particles as the particles are randomly oriented. This approach has been successfully applied on sprays created by standard nozzles [8], including industrial configurations [9].

However, to record fundamental data on heat up and evaporation rate, experiments are often carried out on lines of nearly perfectly monodispersed droplets [10]. By using standard rainbow, measurements are only possible on a finite distance after the injection, limiting the measurement to small residence time.

The aim of this paper is to study the possibility to use global rainbow technique to measure the properties of line of

non spherical droplets. A special attention is devoted to the comparison of size measurements carried out by three different optical techniques: PDA, Shadow imaging and global rainbow.

The paper is organized as follows. The next section displays the experimental setup, including a short presentation of the processing strategies. Then typical rainbow signals are presented for different level of droplet sphericity. Finally the measured size distributions are compared and discussed.

EXPERIMENTAL SETUP

Droplets generation

Droplets are generated by using a vibrating orifice. The nominal droplet diameter is a function of: the orifice diameter, the flow rate and the excitation frequency. The main part of the nozzle can be regulated in temperature, permitting to adjust the temperature of the droplets from 5°C to 80°C. The droplets are injected in a steady air at 23°C. The measurement point is located at 20 mm for the generator orifice. The orifice diameter is equal to 50 µm, the flow rate to 4.0 cc/min and the excitation frequencies used run from 13 kHz to 19 kHz. The droplet velocity is typically equal to 5-7 m/s.

The experimental procedure is as follow:

1. A line of spherical droplets is created, at a given frequency,
2. Then the excitation frequency is changed, generating droplets with a level of non sphericity.
3. Size distributions are measured by GRT, PDA and shadow imaging for both cases

PDA

The "Dual Mode" PDA from DANTEC Company is used. The signal is processed by a BSA P80 processor. The laser source is an Argon-ion laser (Coherent Innova 300C), with a maximum power equal to 10 W. The focal length of the emitting unit is equal to 500 mm and the collecting unit focal length is equal to 310 mm. With such a configuration, the range of measurable diameters runs from 0 to 250 µm.

Shadow Imaging

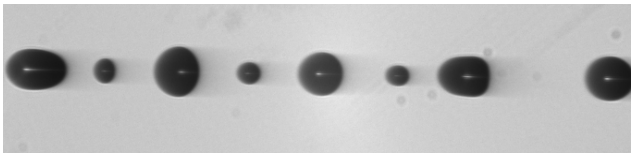

Figure 1: an exemple of a line of non spherical droplets.

The shadow imaging setup is based on the use of white light pulse. The temporal duration of the light pulse is equal to 5 µs (stroboscope MVS-2611). The images created by the use of a long distance microscope (Infinity K2/S) are recorded by a numerical camera (KAPPA 1050x1450 pixels). For the working conditions used in this paper, about 6-8 droplets are visible on each image. An image processing software has been developed to extract the following parameters from images and thus characterise each droplet: diameter, sphericity, ellipticity, irregularity and uniformity. These parameters are defined by using the notion of *perfect disk*. The perfect disk is the disk with the same barycentre and surface than the 2D image of the droplet under study. The parameters are defined as:

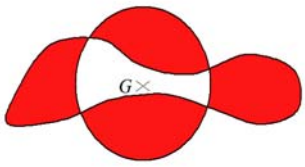

Figure 2: Sphericity (Sp): the aera of the non comon surface divded by the area of the perfect disk.

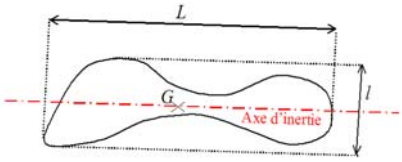

Figure 3: Ellipticity (ε): the ratio small length on long length.

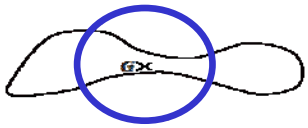

Figure 4: Irregularity (φ) : perfect disk perimeter length over drop perimeter length ratio

Figure 5: Uniformity (η): difference between the maximum and minimum radius over perfect disk radius

For a perfectly spherical droplet, these parameters have the following values: Sp = 0, ε=1, φ=1, η=0.

Global rainbow setup and processing

Figure 6 displays the global rainbow set up. The setup characteristics are the following:

- The collecting focal lenght is equal to 50 mm
- A spatial filter with a diameter equal to 1mm gives the possibility to select a control volume equal to typically 500 µm^3.
- A second lens with a focal lenght equal to 100 mm conjugates the collecting lens image focal plan on the detector aera.
- The image is recorded by a CCD camera KAPPA 1050x1450 Pixels
- A PC records and processes the image

The figure 7 is a typical example of a global rainbow recorded from a line of perfectly spherical droplets

Figure 6: the Global rainbow setup developed at Rouen.

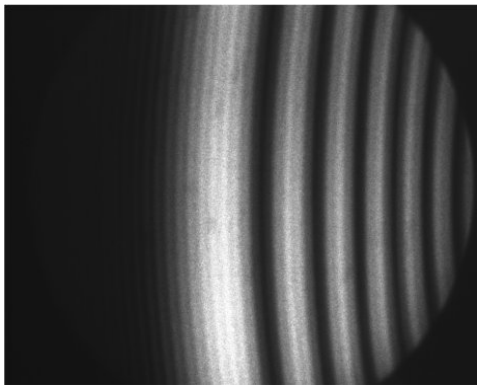

Figure 7: a typical global rainbow recorded from a line of spherical droplets.

Devices connection

The timing of the different devices are controlled by a delay generator (BNC 565) in such a way that the same droplets are analyzed by the different techniques. Typically, the pulses delivered by the delay generator have a frequency 10000 times smaller than the excitation frequency: as only one image by second can be recorded from the shadow imaging setup. Thus, the PDA can be used to measure the velocity and size distribution continuously or by series of 6-8 particles corresponding to the particle recorded by the shadow image setup.

RAINBOW SIGNALS

When the droplets are viewed as spherical, the recorded rainbows look as the one displayed in Figure 7. Such rainbows are characterized by a high degree of symmetry relatively to the horizontal axis. When the droplets shape is modified by changing the excitation frequency, the rainbow behavior is more complex. When highly steady reproducible orientations are obtained, the recorded rainbows lost their symmetry relatively to the horizontal axis. The two images displayed in figure 8 are typical of such situations. In these cases no measurements are possible. In figure 8.a, the rainbow topology is completely lost. In figure 8.b, the global topology is conserved; nevertheless this figure is characterized by phase jumps in the supernumerary bows organization. Such non symmetrical signals have been rejected in the processing procedure.

Refractive index (temperature) processing

Figure 9 displays three global rainbows recorded for three excitation frequencies: 18 kHz, 16 kHz and 13 kHz respectively. Spherical droplets are created at 18 kHz, while non spherical droplets are created at frequencies of 16 kHz and 13 kHz. The deformation of the particles increases as the excitation frequency decreases. In red, for a frequency equal to 18 kHz, the ripple structure is clearly visible. For 16 KHz, the main modification is the lost of the ripple structure while for 13 kHz the supernumerary bows are nearly invisible.

These global rainbow scattering diagrams must be inversed to obtain the refractive index and the size distribution of the droplets. The processing is based on the use of the Non Negative Least Square method, where the elements of the matrix to inverse are computed in the framework of the Nussenzveig's theory [11].

The inversion of these three curves gives the same refractive index value, corresponding to the injection temperature 24°C, independently of the droplet shape. The inversion procedure and the temperature measurement accuracy are exhaustively described elsewhere [11, 12]. In this paper we focus our attention on the size distribution analysis.

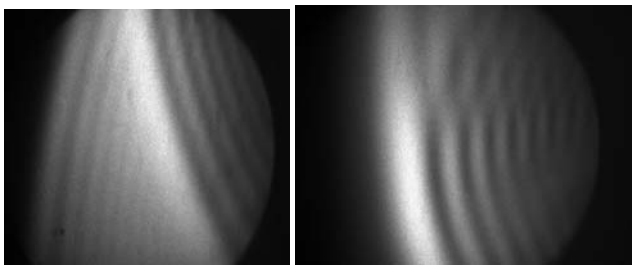

(a) (b)

Figure 8: Typical rainbow recorded for spheroid without random orientation.

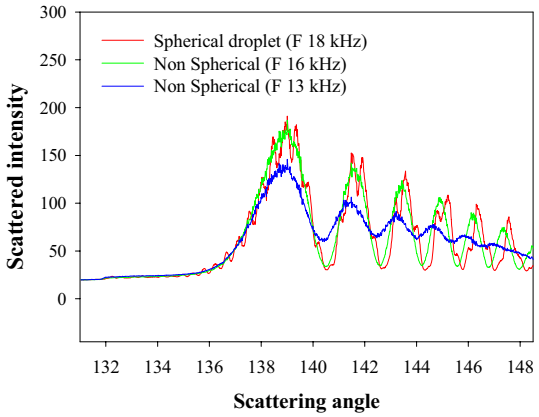

Figure 9: Global rainbow patterns for frequencies excitation equal to 13, 16 and 18 kHz.

SIZE MEASUREMENTS

When working with lines of monodispersed droplets, the velocity of the droplets is measured. This velocity measurement permits to transform the measurement location along the droplets line to resident time and also to characterize the droplet line stability. Figures 10 and 11 display the longitudinal and transverse velocities for different excitation frequencies. The radial velocity is exactly the same for the three excitation frequencies; the droplets are always aligned. Tthe longitudinal velocities are very close: 5.96±0.05 m/s, 5.77±0.03 m/s and 5.665±0.007 m/s for excitation

frequencies equal to 13, 16 and 18 kHz respectively. Furthermore, the important fact is that the velocity standard deviation increases as the excitation frequency decreases.

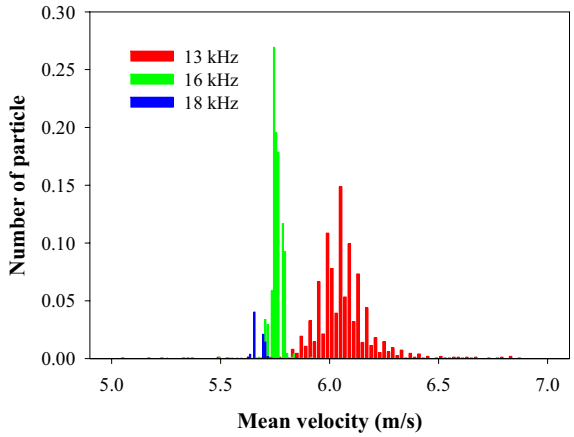

Figure 10: Droplet longitudinal velocity for excitation frequencies excitation equal to 13, 16 and 20 kHz.

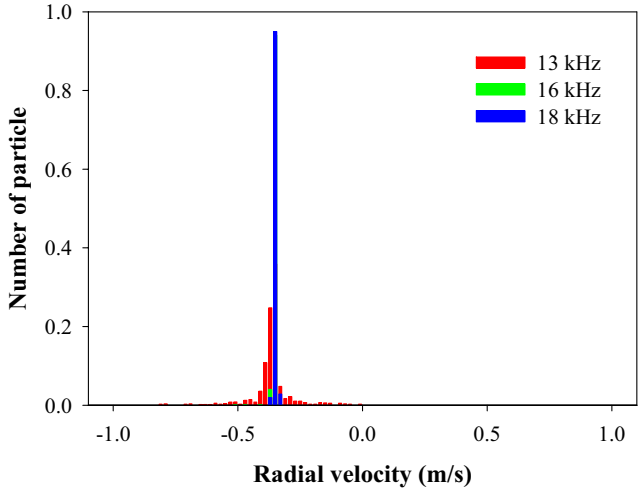

Figure 11: radial velocity for excitation frequencies equal to 13, 16 and 18 kHz.

This increasing of the longitudinal standard deviation velocity can be directly connected to the droplet non sphericity. Figure 12 displays diameter size distribution measured by shadow imaging. For the three excitation frequencies, the mean diameter is around 100 µm. For 16 and 18 kHz the size distribution is relatively narrow, but for 13 kHz the size distribution is very large.

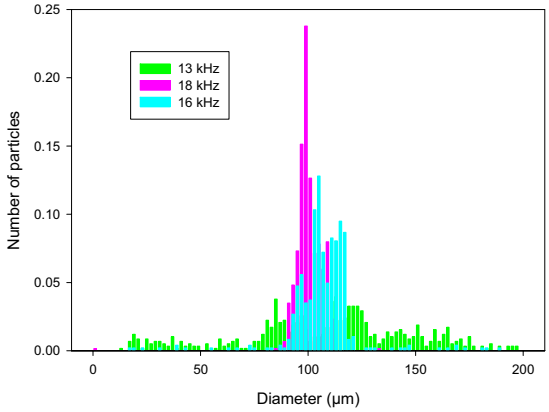

Figure 12: Size distribution obtained from shadow imaging for excitation frequencies equal to 13, 16 and 18 kHz.

This behaviour is in agreement (qualitatively) with PDA measurements. The size distribution measured by PDA are plotted in figure 13. At the scale this figure, the size distribution for excitation frequencies equal to 18 and 16 kHz looks monodispersed and close with a mean diameter equal to about 115 µm. For an excitation frequency equal to 13 kHz, the size distribution measured by PDA is clearly bimodal. The two peaks corresponds to diameters equal to about 98 µm and 120 µm. According with the works of Damaschke et al [13], such a bimodal distribution is typical of PDA measurements with non spherical droplets. Figure 14 presents a zoom of figure 13 for excitation frequencies equal to 16 and 18 kHz. At this scale, it is clear that for an excitation equal to 16 kHz, the size distribution measured by PDA is also bi-modal. The two peaks are close (117 and 118 µm), but clearly separated while for an excitation equal to 18 kHz, only one peak has been measured by PDA, corresponding to a diameter equal to about 112 µm. The main differences between imaging and PDA size distributions are only that imaging size distributions have a larger standard deviation and underestimate the mean diameter.

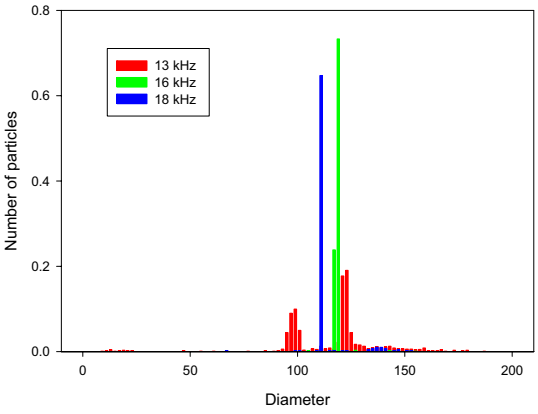

Figure 13: Comparaison of size distribution measured by global rainbow and PDA technique

Figure 15 displays the measured size distribution by GRT for different frequencies. By comparing with figures 13 and 14, it is clear that size measurements by PDA and GRT are in good agreement for excitation frequencies equal to 16 kHz and 18 kHz. On the contrary for the case of 13 kHz, corresponding to the most deformed droplets, the disagreement is dramatic. The global rainbow size distribution is nearly exclusively composed of small droplets

(less than 15 µm) while PDA measurements are around 110 µm. However, these distributions are in number. Therefore, volume weighted size distributions have been displayed in Figures 16 and 17 for GRT and PDA measurements respectively. For PDA measurements, the change is minor while for GRT the relative contribution of the small droplets is considerabely reduced. Both techniques give the comparable mean size (in volume).

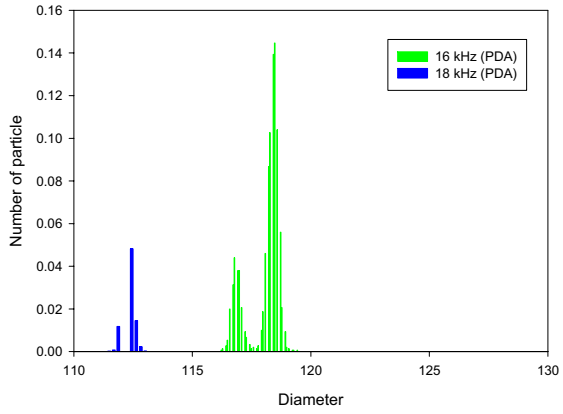

Figure 14: Comparaison of size distribution measured by global rainbow and PDA technique

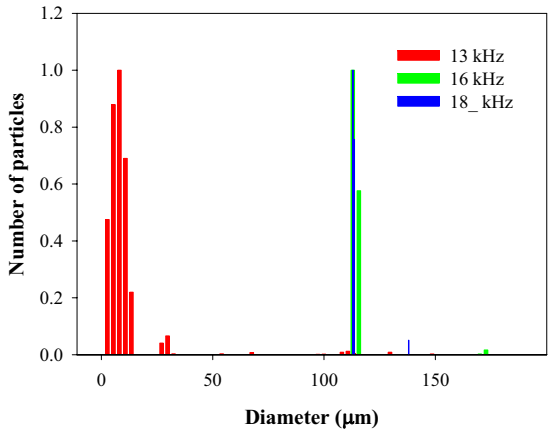

Figure 15: Comparison of size distribution (in number) measured by GRT and PDA.

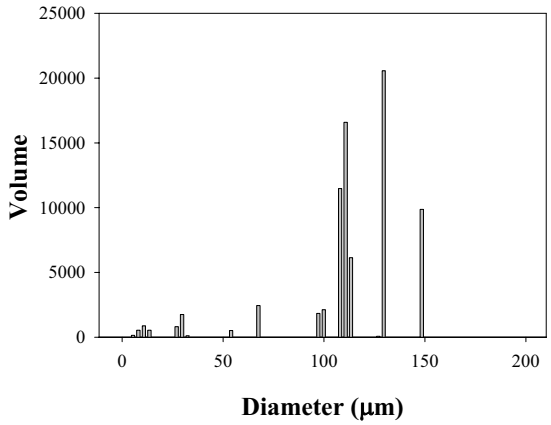

Figure 16: Volume by class of diamter from Global rainbow technique

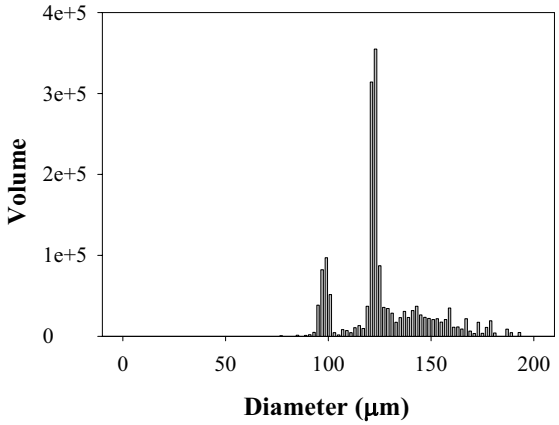

Figure 17: Volume by class of diameter from PDA technique.

The overestimation of the number of small particles in global rainbow measurements, when the scatterering droplets are not perfectly spherical, can be understand as follow:

- During the recording, non spherical droplets scatter light in angular regions where spherical droplets can not, as in the Alexander's dark band (due to a negative shift of the rainbow as predicted by Nobiüs [14]).
- During the inversion process, to fit the recorded light intensity profile, the code creates 'ghost' small spherical droplets. Only these small particles are able to scatter light in forbidden regions as in the Alexander's dark band with a very low intensity. Then to reach the intensity level recorded in forbidden regions, the code proposes a huge number of small spherical droplets.

CONCLUSION

It has been experimentally demonstrated by the Global rainbow technique can be successfully applied to line of droplets.

When the droplets are perfectly spherical, both the refractive index and the size distribution (reduce to one peak of course) are perfectly extracted. The refractive index measurement accuracy corresponds to few degrees on water droplets while the size measurements are in agreement with PDA and shadow imaging measurements.

When the droplets are not perfectly spherical, the droplets orientation must be sufficiently random to create symmetrical 'rainbows'. From such rainbows, the refractive index is easily extracted with accuracy. The extraction of the size distribution is more difficult due to the creation of ghost small droplets by the inversion code. Only measurement of volume weighed distribution can be expected.

ACKNOWLEDGMENT

This work is supported by the CNRS/ONERA program ASTRA.

NOMENCLATURE

Symbol	Quantity	SI Unit
GRT	Global Rainbow Technique	
IR	Infra Red	
LIF	Laser Induced fluorescence	
MDR	Morphological dependent resonances	

PDA	Phase Doppler Anemometer
Sp	Sphericity
ε	Ellipticity
φ	Irregularity
η	Uniformity

REFERENCES

[1] G. Chen, Md. M. Mazunder, R.K. Chang, J.C. Swindal and W.P. Acker, Laser diagnostics for droplet characterization: application of morphology dependent resonances, Prog. Energy Combust. Sci, 22, 163--188, 1996

[2] P. Lavieille, F. Lemoine, G. Lavergne and M. Lebouche, M., Evaporating and combusting droplet temperature measurements using two-color laser-induced fluorescence, Experiments in Fluids, 31, 45-55, 2001

[3] C. Amiel, Application de techniques optiques à l'étude du comportement dynamique et thermique de gouttes en interaction avec une paroi chauffée, PhD Ecole Nationale Supérieure de l'Aéronautique et de l'espace, Toulouse, France, 2003

[4] T. Müller, G. Grünefeld and V. Beushausen, High-precision measurement of the temperature of methanol and ethanol droplets using spontaneous Raman scattering. Appl. Phys. B, 70, 155-158, 2000.

[5] J. Wilms, Evaporation of multicomponent Droplets, PhD thesis, Universitat Stuttgart, October, 2005

[6] P.L. Marston, Rainbow phenomena and the detection of nonsphericity in drops, Applied Optics, 19, 680--685, 1980

[7] J.P.A.J. van Beeck, D. Giannoulis, L. Zimmer and M.L. Riethmuller, Global rainbow refractometry for droplet temperature measurement, Optics Letters, 24, 1696-1698, 1999

[8] M.R. Vetrano, J.P.A.J. van Beeck and M.L. Riethmuller, Global rainbow thermometry: improvement in the data inversion algorithm and validation technique in liquid-liquid suspension, Applied Optics, 43, 3600-3607, 2004

[9] P. Lemaitre, E. Porcheron, G. Grehan and L. Bouilloux, Development of a global rainbow refractometry technique to measure the temperature of spray droplets in a large containment vessel., Meas. Sci. Technol., 17, 1299-1306, 2006

[10] J.F. Virepinte, Etude du comportement dynamique et thermique de gouttes en regimes d'interaction dans le cas de jets rectilignes, Thèse de doctorat, Ecole Nationale Supérieure de l'Aéronautique et de l'Espace, 1999

[11] S. Saengkaew, Development of novel global rainbow technique for characterizing spray generated by ultrasonic nozzle. PhD thesis of Chulalongkorn University, Bangkok (Thailand), 2005.

[12] S. Saengkaew, G. Godard, J.B. Blaisot and G. Gréhan, Refractive index measurements by Global rainbow refractometry for spherical and non spherical droplets. Lisbon 2008, ??-?? July.

[13] N. Damaschke, G. Gouesbet, G. Grehan, H. Mignon and C. Tropea, Responde of phase Doppler anemometer systems to nonspherical droplets, Applied Optics, 37, 10, 1752-1761, 1998.

[14] W. Mobiüs, Theorie des regenbogens unnd ihrer experimentellen prufung, Annalen der Physik, IV, 1498-1558, 1911.